Plasmon Resonance Studies of Agonist/Antagonist Binding to the Human δ-Opioid Receptor: New Structural Insights into Receptor-Ligand Interactions

Z. Salamon,* S. Cowell,† E. Varga,‡ H. I. Yamamura,*‡ V. J. Hruby,*† and G. Tollin*†
Departments of †Chemistry, *Biochemistry, and ‡Pharmacology, University of Arizona, Tucson, Arizona 85721 USA

ABSTRACT Structural changes accompanying the binding of ligands to the cloned human δ-opioid receptor immobilized in a solid-supported lipid bilayer have been investigated using coupled plasmon-waveguide resonance spectroscopy. This highly sensitive technique directly monitors mass density, conformation, and molecular orientation changes occurring in anisotropic thin films and allows direct determination of binding constants. Although both agonist binding and antagonist binding to the receptor cause increases in molecular ordering within the proteolipid membrane, only agonist binding induces an increase in thickness and molecular packing density of the membrane. This is a consequence of mass movements perpendicular to the plane of the bilayer occurring within the lipid and receptor components. These results are consistent with models of receptor function that involve changes in the orientation of transmembrane helices.

INTRODUCTION

The majority of transmembrane signal transduction responses to hormones, neurotransmitters, phospholipids, photons, odorants, and growth factors are mediated by a superfamily (containing nearly 2000 members and growing) of seven transmembrane helical G-protein-coupled receptors (GPCRs). Activation of these receptors by external stimuli is assumed to require protein conformational changes. Current methods used to examine ligand-binding interactions with such GPCRs, as well as with other membrane-bound receptors, suffer from several deficiencies. These include the use of radiolabeled ligands, which require special synthetic methodologies, and present special disposal and potential toxicity problems. In some cases, ligands with fluorescent probes can be used, but the modification of the ligand by the fluorophore often leads to changes in the binding and other physical/chemical properties of the ligand. Perhaps most importantly, current binding methods, whether using radiolabeled or fluorescent-labeled ligands, provide no information regarding the changes in receptor structure that accompany ligand-receptor interactions, nor do they distinguish the different structural changes that occur for agonists and antagonists interacting with the same receptor.

We report herein results obtained with a new method employing plasmon resonance spectroscopy that can monitor the binding interaction of peptide ligands with a GPCR. The information thereby obtained includes the direct determination of the thermodynamic binding constant for the noncovalent ligand-receptor interaction and an assessment of the structural changes that accompany this interaction, all in a single, highly sensitive measurement using unmodified materials. The procedure utilizes a newly developed variant of the surface plasmon resonance (SPR) technique referred to as coupled plasmon-waveguide resonance (CPWR) spectroscopy (Salamon et al., 1997a, 1999; Salamon and Tollin, 1999a, 2000), which allows the characterization of anisotropic membrane systems (Salamon et al., 1997a, 1998, 1999), as well as other anisotropic nanostructures (Salamon and Tollin, 1999b, 2000). This methodology has the unique capability of independently examining real-time changes in the structure of the receptor both parallel and perpendicular to the lipid membrane plane in response to receptor-ligand interactions (Salamon et al., 1999). CPWR also provides greatly enhanced sensitivity and spectral resolution compared to conventional SPR. As will be demonstrated below, only femtomole amounts of receptor (and ligand) are needed for complete spectral determination and analysis. Furthermore, because radioactivity measurements do not have to be performed, the methodology is much more rapid and direct in the determination of critical binding parameters. CPWR spectroscopy thus provides a general procedure that we believe can replace previous methods for examining ligand-membrane-bound receptor interactions, and which at the same time can provide new information about ligand-receptor structural transitions that are not available with these methodologies.

In the present report, we illustrate this procedure via incorporation of the human δ-opioid receptor into a preformed lipid bilayer, examination of the binding to the receptor of the highly selective ligand DPDPE (*c*-[D-Pen^2, D-Pen^5] enkephalin; Mosberg et al., 1983), demonstration of the reversal of binding using the selective antagonist naltrindol (NTI; Raynor et al., 1994; Korlipara et al., 1995), and evaluation of the changes in the receptor structure that accompany these binding interactions. We present clear evidence that significantly different structural changes are induced in the δ-opioid receptor upon binding of either

Received for publication 8 March 2000 and in final form 16 August 2000.
Address reprint requests to Dr. Gordon Tollin, Department of Biochemistry, University of Arizona, Tucson, AZ 85721. Tel: 520-621-3447; Fax: 520-621-9288; E-mail: gtollin@u.arizona.edu.

0006-3495/00/11/2463/12 $2.00

DPDPE or NTI, thereby providing new insights into the structural basis of receptor function.

EXPERIMENTAL PROCEDURES

Purification of the receptor

The human brain δ-opioid receptor (accession number U07882; Knapp et al., 1994) mediates analgesic responses to endogenous enkephalins as well as to a variety of synthetic agonists. A fully functional receptor, labeled at the C terminus with a *myc* epitope (Gimpl et al., 1996) and His tag (Grisshammer and Tucker, 1996), was prepared by inserting the DNA of the human δ-opioid receptor, which was modified by incapacitating the stop codon of the receptor, into the pcDNA3 vector containing the *myc*/His tag (Invitrogen). The entire vector was verified by DNA sequencing and stably transfected into a Chinese hamster ovary cell line with the use of diethylaminoethyl-dextran (Promega). The transfected clones were selected using G418 as an antibiotic. These were grown to confluency in Hamm's F12 medium with 10% fetal bovine serum containing penicillin (100 units/ml) and streptomycin (100 μg/ml) in a humidified CO_2 atmosphere at 37°C. Related experiments characterizing the modified receptor have been carried out (Okura et al., 2000).

After the cells were harvested and washed several times, they were suspended in Tris-Cl buffer at pH 7.4 and centrifuged at 42,000 rpm (160,000 × *g*) at 4°C for 30 min. The buffer was decanted and the membranes were solubilized by homogenization in a solution containing 25 mM HEPES, 0.5 M KCl, 30 mM octylglucoside, and protease inhibitors designed to be used with metal chelating columns (Sigma) (buffered at pH 7.4). After homogenization the solution was centrifuged at 42,000 rpm again for 60 min to remove cell debris.

The receptor was purified on a Talon Co^{2+} metal chelating column (Clontech) with gentle rocking for 48 h at 12°C and eluted with 25 mM HEPES, 0.5 M KCl, 30 mM octylglucoside, and 100 mM imidazole buffered at pH 7.4. Although the binding can be carried out in 24 h, this experiment was allowed to go for 48 h to maximize binding of the receptor to the Talon column. The column and receptor homogenate were kept at 12°C to minimize any possible denaturation of the receptor due to heat or protease, which may still be present in the system. The concentration of receptor in the purified sample was determined in a binding assay using a radioactive ligand (Okura et al., 2000).

The agonist (DPDPE) used in this work was synthesized in Dr. Victor Hruby's laboratory (Mosberg et al., 1983), and the antagonist (NTI) was obtained from RBI Labs.

Formation of solid-supported lipid bilayers

Self-assembled solid-supported lipid membranes were prepared according to the method used for the formation of freely suspended lipid bilayers (Mueller et al., 1962). This involves spreading a small amount of lipid solution across an orifice in a Teflon sheet that separates the thin dielectric film (SiO_2) from the aqueous phase (Salamon et al., 1999). The hydrophilic surface of hydrated SiO_2 attracts the polar groups of the lipid molecules, thus inducing an initial orientation of the lipid molecules, with the hydrocarbon chains pointing toward the droplet of excess lipid solution. The next steps of bilayer formation, induced by adding aqueous buffer to the sample compartment of the CPWR cell, involve a thinning process and the formation of a plateau-Gibbs border of lipid solution that anchors the membrane to the Teflon spacer. In the present experiments, the lipid films were formed from a solution containing 5 mg/ml egg phosphatidylcholine (PC) and 1-palmitoyl-2-oleoyl-*sn*-glycero-3-[phospho-*rac*-(1-glycerol)(sodium salt) (POPG) (75:25 mol/mol) in squalene/butanol/methanol (0.05:9.5:0.5, v/v). The lipids were purchased from Avanti Polar Lipids (Birmingham, AL). All experiments were carried out at ambient temperature, using 10 mM Tris buffer containing 0.5 mM EDTA and 10 mM KCl (pH 7.3), in the 2-ml sample cell.

CPWR spectroscopy

Details of the procedures for CPWR measurement and data analysis have been described elsewhere (Salamon et al., 1997a, 1999; Salamon and Tollin, 1999a). The method is based upon the resonant excitation by polarized light from a CW He-Ne laser (λ = 632.8 nm), passing through a glass prism under total internal reflection conditions, of collective electronic oscillations (plasmons) in a thin metal film (Ag) deposited on the external surface of the prism, which is overcoated with a dielectric layer (SiO_2). The resonant excitation of plasmons generates an evanescent electromagnetic field localized at the outer surface of the dielectric film, which can be used to probe the optical properties of molecules immobilized on this surface (for details see Salamon et al., 1997a, 1999; Salamon and Tollin, 1999a, 2000). Resonance is achieved either by varying the incident-light wavelength (λ) at a fixed incident angle (α), or by varying α at a fixed λ (in the present experiments the latter protocol was used). Because the resonance coupling generates electromagnetic waves at the expense of incident light energy, the intensity of totally reflected light is diminished. The reflected light intensity as a function of either λ or α results in a CPWR resonance spectrum. The resonance can be excited with light polarized either parallel (*p*) or perpendicular (*s*) to the incident plane, resulting in two well-separated spectra (Salamon et al., 1997a), thereby allowing characterization of the molecular organization of anisotropic systems such as biomembranes containing integral proteins (Salamon et al., 1994, 1996, 1998, 1999). Under the experimental conditions employed in this work the optical parameters obtained with *p*-polarization refer to the perpendicular direction, and those obtained with *s*-polarization to the parallel direction, relative to the bilayer membrane surface.

CPWR spectra can be described by three parameters: α (or λ), the spectral width, and the resonance depth. These depend on the refractive index (n), the extinction coefficient (k), and the thickness (t) of the plasmon-generating and emerging media, the latter including a thin film deposited on the silica surface (i.e., a proteolipid membrane in the present case) in contact with an aqueous solution. Thin-film electromagnetic theory based on Maxwell's equations provides an analytical relationship between the spectral parameters and the optical properties of these media. This allows evaluation of n, k, and t uniquely for the three media (i.e., the plasmon-generating medium, the proteolipid membrane, and the aqueous buffer solution), by nonlinear least-squares fitting of the theoretical spectrum to the experimental one (for details see Salamon et al., 1997b, 1998, 1999, 2000; Salamon and Tollin, 1999b). Inasmuch as the excitation wavelength (632.8 nm) is far removed from the absorption bands of the lipids, protein, and ligands used in this work, a k value other than zero reflects a decrease in reflected light intensity due only to scattering resulting from imperfections in the proteolipid film. This effect will not be discussed further in the present work.

It is important to point out that for an anisotropic thin film, such as the proteolipid membrane in the present work, the thickness (t) represents an average molecular length perpendicular to the plane of the film and will be independent of light polarization. In contrast, the values of the refractive index (n) will be very much dependent on the polarization of the excitation light. Furthermore, for uniaxial anisotropic structures in which the optical axis is parallel to the *p*-polarization direction, the n_p value will always be larger than n_s. This is a consequence of the fact that the measured refractive index of a material is determined by the polarizability of the individual molecules. The latter property describes the ability of a molecule to interact with an external electromagnetic field and in general is anisotropic with respect to the molecular frame. In the simplified case in which the molecular shape is rod-like (e.g., the phospholipid molecules used in this work), one can assign two different values to the polarizability: the larger one, which is longitudinal, and the smaller one, which is transverse. If, in addition to the anisotropy in molecular shape and polarizability, the system

that contains these molecules is ordered such that the long axes of the molecules are parallel, this results in long-range order usually described by the order parameter *S*. In this situation the values of the polarizability, averaged over the whole system and measured either parallel or perpendicular to the direction of the long axes of the molecules, will be different (i.e., the parallel value will be larger than the perpendicular one). These conditions create an optically anisotropic system, with the optical axis perpendicular to the plane of the proteolipid membrane, and the values of the refractive index measured with two polarizations of light (i.e., parallel, n_p, and perpendicular, n_s, to the optical axis) will describe this optical anisotropy (A_n) as follows:

$$A_n = (n_p^2 - n_s^2)/(n_{av}^2 + 2) \quad (1)$$

In this equation n_{av} is the average value of the refractive index and, for a uniaxial system, is given by

$$n_{av}^2 = 1/3(n_p^2 + 2n_s^2) \quad (2)$$

In summary, the anisotropy in the refractive index reflects both the anisotropy in the molecular polarizability and the degree of long-range order of molecules within the system and therefore can be used as a tool to analyze structural organization (i.e., molecular orientation). This is particularly important in the context of the present work, in which structural alterations of a proteolipid membrane (consisting of a single lipid bilayer with inserted receptor molecules) caused by ligand binding have been monitored by changes in the refractive index anisotropy. A more quantitative discussion of this will be presented separately (Salamon and Tollin, manuscript in preparation).

Furthermore, as can be seen from the Lorentz-Lorenz relation, the average value of the refractive index is also directly related to the mass density (for details see Born and Wolf, 1965; Cuypers et al., 1983). Thus, from the thickness of the proteolipid film and the average value of the refractive index one can calculate the surface mass density (or molecular packing density), i.e., mass per unit surface area (or number of moles per unit surface area; Salamon et al., 1999; Salamon and Tollin, 1999a, 2000).

In the present experiments, the plasmon-generating device was calibrated by measuring the CPWR spectra obtained from a bare silica surface in contact with aqueous buffer with both *p*- and s-polarized light and then fitting these with theoretical curves. The goal of such a calibration is to obtain the optical parameters of the silica layer (i.e., refractive indices, extinction coefficients, and thickness) used in these experiments. This provides an input set of data used in analyzing the resonance spectra obtained with proteolipid membranes deposited on the silica surface. Thus the resonance spectra obtained after a single lipid bilayer membrane was created on the hydrophilic surface of silica were fit using these data, yielding the optical parameters (n_p, n_s, and t) for the lipid bilayer. These allowed the calculation of the refractive index anisotropy and the surface mass density (i.e., molecular packing density) of the bilayer. After incorporation of the receptor molecules into the lipid membrane, the resulting CPWR spectra allowed us to characterize the structural consequences of receptor incorporation. Finally, addition to the aqueous sample compartment of the CPWR cell of either agonist or antagonist again resulted in changes of the CPWR spectra, which reflected structural alterations in the proteolipid membrane caused by the receptor-ligand interaction.

RESULTS AND DISCUSSION

Incorporation of the δ-opioid receptor into a preformed lipid bilayer

Receptor molecules were incorporated into a preformed lipid membrane deposited on the hydrophilic surface of the silica film by adding small aliquots of a concentrated solution of the human δ-opioid receptor solubilized in 30 mM octylglucoside to the aqueous compartment of the CPWR cell, thereby diluting the detergent to a final concentration below its critical micelle concentration (25 mM) (Salamon et al., 1994, 1996). This resulted in spontaneous transfer of the receptor from the micelle to the lipid bilayer. The direction of insertion of the receptor in the bilayer is not known. However, as will be shown below, ligand binding to the incorporated receptor occurs efficiently.

Fig. 1 shows typical CPWR spectra, obtained with either *p*-polarized (Fig. 1 *A*) or *s*-polarized (Fig. 1 *B*) exciting light, for a solid-supported lipid membrane before (*curve 1*)

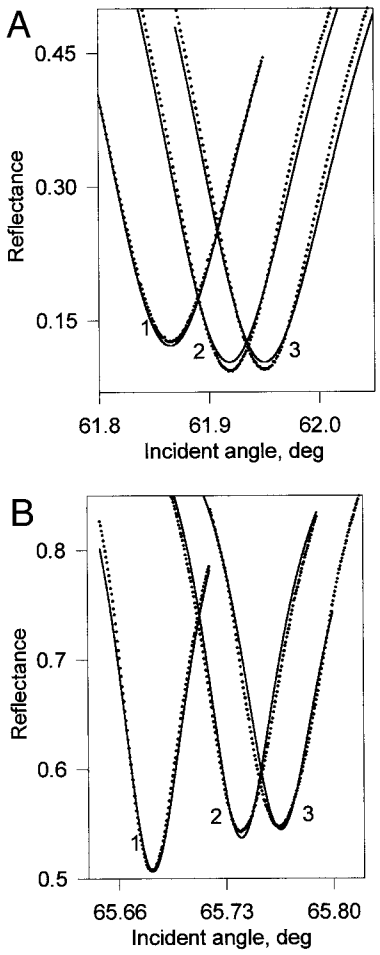

FIGURE 1 CPWR spectra obtained for a supported lipid bilayer containing 75 mol% egg phosphatidylcholine and 25 mol% phosphatidylglycerol before (*curve 1*) and after the addition of aliquots of human δ-opioid receptor in octylglucoside-containing buffer to the aqueous compartment of the CPWR cell (the final receptor concentration in the bulk solution for *curve 2* was 4.8 nM, and that for *curve 3* was 12.8 nM). The buffer composition was 10 mM Tris (pH 7.3), 0.5 mM EDTA, and 10 mM KCl. The octylglucoside concentration in the receptor solution was 30 mM; after dilution into the sample cell the concentration ranged from 0 to 5 mM. Data obtained with *p*-polarized (*A*) and *s*-polarized (*B*) exciting light are shown. Dotted lines represent theoretical fits. The refractive index and thickness values obtained from these fits are given in Fig. 4. In all cases, CPWR spectra were obtained after equilibrium was reached (20–40 min).

and after two additions of detergent-solubilized receptor to the aqueous compartment of the sample cell (*curves 2* and *3*). As noted previously with other integral membrane proteins, including rhodopsin (Salamon et al., 1994, 1996), protein incorporation into the bilayer influences all three parameters of the resonance spectrum, i.e., angular position, depth, and spectral half-width. Such changes are due both to mass density changes and to structural alterations of the proteolipid membrane (reflected in changes in refractive index and thickness). These will be considered further below.

Binding of agonist (DPDPE) and antagonist (NTI) to incorporated receptor

In this section we describe the primary spectral data obtained upon adding DPDPE and NTI to the previously incorporated receptor. As will be demonstrated, these data clearly reveal different patterns of receptor-agonist and receptor-antagonist interaction.

When aliquots of either DPDPE or NTI solutions are added to the sample cell after receptor incorporation into a preformed bilayer, significant changes in the position, width, and depth of the CPWR resonance curve occur. These spectral changes reflect the binding of these molecules to the proteolipid membrane. Control experiments involving the addition of comparable amounts of these ligands to a CPWR cell containing a preformed bilayer in the absence of receptor produced no measurable effects on the CPWR spectra (data not shown), indicating that nonspecific binding to the membrane is not detected in these experiments. Thus the spectral changes observed when the receptor is present must reflect receptor-ligand interactions.

To illustrate these changes, examples of resonance spectra obtained with both *p*- and *s*-polarized exciting light are shown in Figs. 2 and 3. Fig. 2 shows the results of an experiment in which agonist is added to the receptor-containing CPWR cell first, followed by antagonist addition, and Fig. 3 shows an experiment in which antagonist is added first, followed by agonist. As can clearly be seen, the effects of these two ligands on the resonance spectra are easily measurable and quite different. Although all three spectral parameters (i.e., position, width, and depth) are significantly altered by both ligands, appreciable differences are seen in the amplitude and direction of the resonance shifts. Thus DPDPE causes much larger changes in

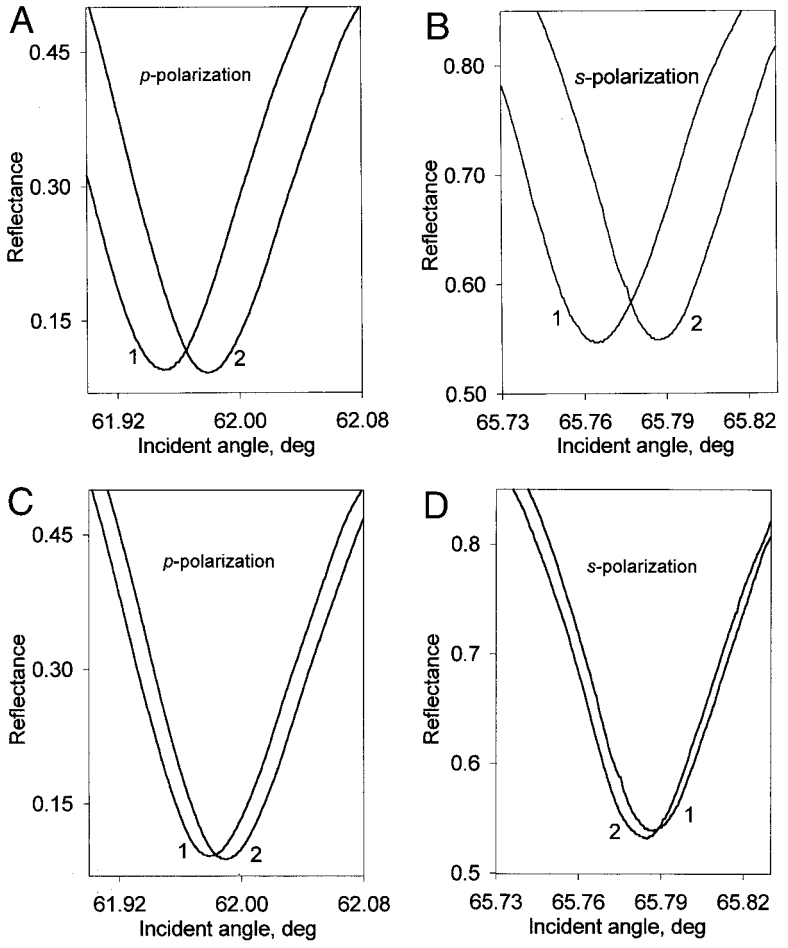

FIGURE 2 CPWR spectra obtained in an experiment in which addition to the aqueous compartment of agonist (DPDPE) is followed by the addition of antagonist (NTI). The cell contained a lipid membrane with the receptor incorporated (the final bulk receptor concentration was 12.8 nM; spectra are shown in *curves 1* in *A* and *B*). *Curves 2* in *A* and *B* show the spectra obtained after the addition of 79 nM DPDPE. *Curves 1* in *C* and *D* are the same as *curves 2* in *A* and *B*. *Curves 2* in *C* and *D* show the spectra obtained after the addition of 0.64 nM NTI. Other conditions are as in Fig. 1.

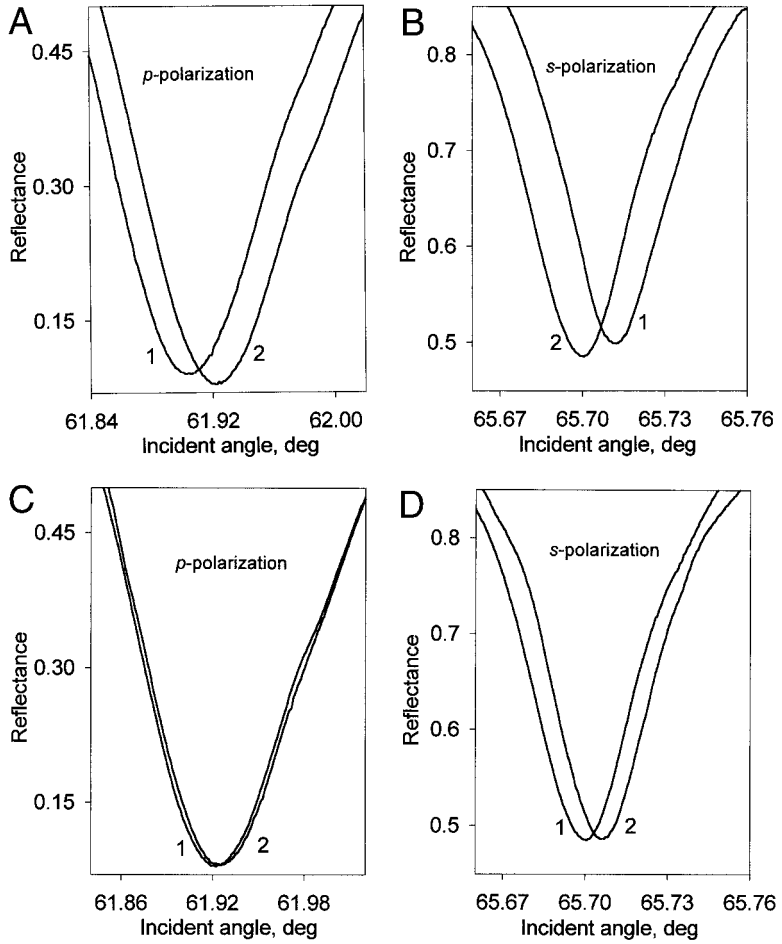

FIGURE 3 CPWR spectra obtained in an experiment in which the addition of antagonist is followed by the addition of agonist. The cell contained a lipid membrane containing the receptor, as in Fig. 2 (the final bulk concentration was 12.8 nM; the spectra are shown in *curves 1*, *A* and *B*). *Curves 2* in *A* and *B* show the spectra obtained after the addition of 0.144 nM NTI. This was followed by the addition of 360 nM DPDPE (*curve 2, C* and *D*). *Curve 1* in *C* and *D* is the same as *curve 2* in *A* and *B*. Other conditions are as in Fig. 1.

both *p*- and *s*-polarized spectra (compare Fig. 2, *A* and *B*, with Fig. 3, *A* and *B*) than are induced by NTI. In addition, DPDPE shifts both resonances to larger incident angle values (see Fig. 2, *A* and *B*, and Fig. 3, *C* and *D*), although the change in the *p*-polarized signal is quite small (see Fig. 5). In contrast, NTI moves the *p*-polarized resonance to larger (see Figs. 2 *C* and 3 *A*) and the *s*-polarized resonance to smaller, incident angles (see Figs. 2 *D* and 3 *B*).

To further illustrate these differences, plots of the resonance position shifts as a function of added concentration of the two ligands are shown in Figs. 4 and 5. These data also illustrate the fact that adding antagonist after agonist does not simply reverse the changes generated by agonist binding (see Fig. 4). In contrast, agonist added after antagonist is bound is able to reverse the changes caused by the receptor-antagonist interaction (as can clearly be seen in the *s*-polarized component in Fig. 5).

It is essential to emphasize that these spectral changes saturate within concentration ranges (0–40 nM for DPDPE (see Fig. 4) and 0–0.1 nM for NTI (see Fig. 5)) that are consistent with literature data for the binding characteristics of the ligands (see discussion below). Thus it is very unlikely that such high binding affinities result from nonspecific receptor-ligand interactions. Furthermore, the results presented in Figs. 4 and 5 also clearly indicate that, although the direction of the shifts remains the same regardless of which ligand is added first, the concentration ranges in which the resonance shifts occur depend on the sequence of addition (compare Figs. 4 and 5). Thus, in the experiments in which agonist is added first, the antagonist concentration range is significantly higher than that for the opposite case. The same observation applies to the agonist when the antagonist is added first. We will return to this point below.

Preliminary time-resolved measurements of the CPWR spectra after ligand addition demonstrate quite different kinetic properties, depending on which ligand is interacting with the receptor. Fig. 6 shows an example of such a time-dependent spectral sequence obtained with DPDPE, using *s*-polarized light. There are two significant features of these spectral changes that distinguish the receptor-agonist interaction from that of the receptor-antagonist interaction. First, agonist addition results in a very slow (on the order of minutes) time course of spectral changes, whereas antagonist addition results in spectral changes that occur faster than the resolution time (~10 s) of the present experiments. Second, the kinetic properties of the spectral alterations

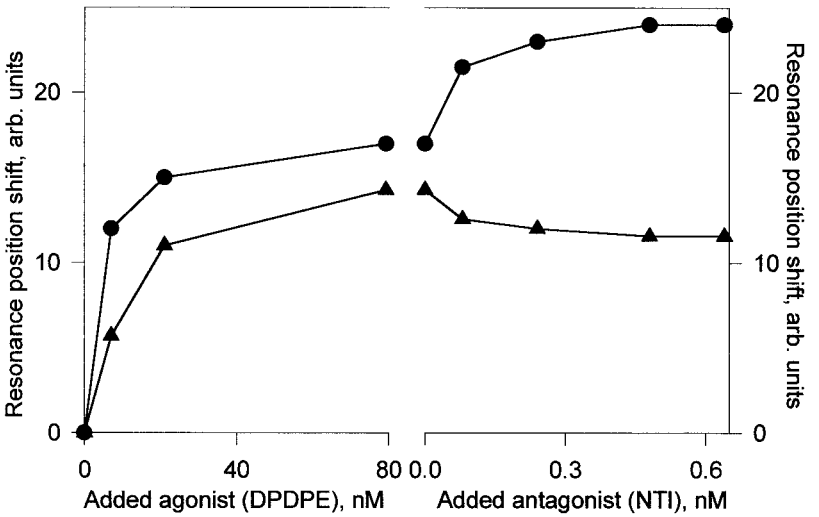

FIGURE 4 Dependence of the relative position of the CPWR resonance minimum on the agonist (DPDPE) and antagonist (NTI) concentrations in the sample compartment of the cell, obtained using either *p*- (●) or *s*- (▲) polarization. Resonance position displacement toward higher values represents shifts to larger angles of incidence. Results were obtained in a continuation of the experiment described in Fig. 2. After receptor incorporation, aliquots of the agonist solution in buffer were added; this was followed by the addition of aliquots of the antagonist solution. Other conditions are as in Fig. 1.

observed with the agonist are quite complicated, involving negative shifts followed by positive shifts in an overall multiphasic process (which we have not characterized in full detail). Such results indicate a complex process of receptor-ligand interaction. It is important to note that a similar complex pattern of spectral changes is observed with the *p*-polarized component (data not shown).

The above-noted differences between agonist and antagonist binding properties cannot be explained simply by differences in either the adsorbed mass of the ligand or its rate of diffusion to the receptor, inasmuch as these ligands have similar molecular masses (i.e., 648 for DPDPE and 414 for NTI). Furthermore, preliminary experiments using another highly selective δ-opioid agonist, deltorphin II (Tyr-D-Ala-Phe-Glu-Val-Val-Gly-NH_2; data not shown), reveal a kinetic pattern similar to that observed with DPDPE. It is also important to note that the present data for the δ-opioid receptor show striking parallels to recent studies with the β_2 adrenergic receptor, in which fluorescence spectroscopy was used to delineate structural changes associated with receptor-ligand interaction (Gether et al., 1997). In these experiments the time course of fluorescence clearly demonstrated that the kinetics of the receptor-agonist interaction are very comparable to those observed in the present study (Fig. 6, *inset*), showing slow (on the order of minutes) multiphasic kinetics, whereas the receptor-antagonist interaction is much faster and simpler.

Although it is clear that further time-resolved studies are necessary to fully understand the complexity of the receptor-agonist interaction process (such studies are presently under way), it is possible to conclude from the present data that the interaction of the δ-opioid receptor with agonist or antagonist generates different structural states of the proteolipid membrane, the properties of which depend on the sequence of ligand addition. To provide a quantitative description of such states it is necessary to analyze the spectral

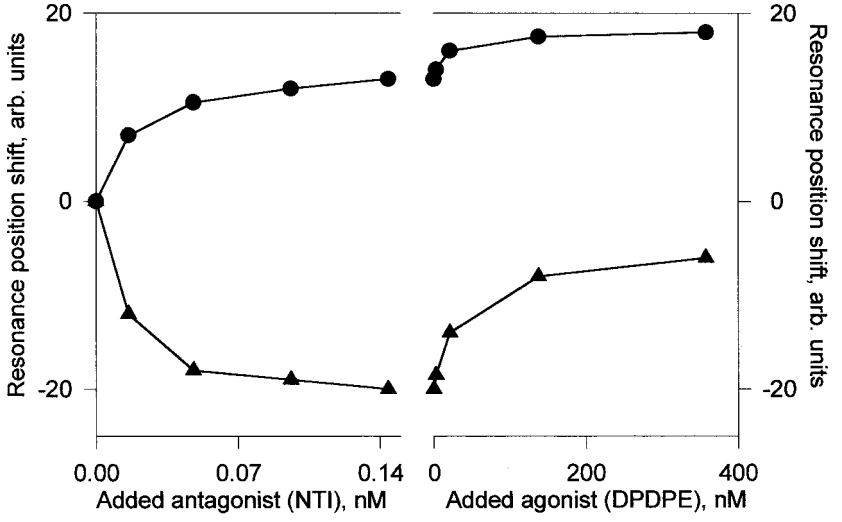

FIGURE 5 Dependence of the relative position of the CPWR resonance minimum on the antagonist (NTI) and agonist (DPDPE) concentration in the sample compartment of the cell, obtained using either *p*- (●) or *s*- (▲) polarization. Resonance position displacement toward higher values represents shifts to larger angles of incidence. Results were obtained in a continuation of the experiment described in Fig. 3. After receptor incorporation, aliquots of antagonist solution in buffer were added; this was followed by the addition of agonist solution. Conditions are as in Fig. 1.

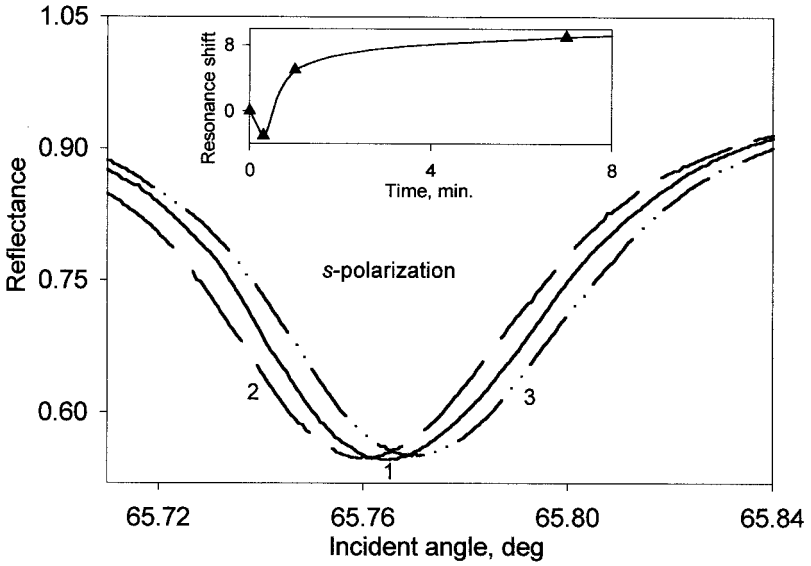

FIGURE 6 CPWR time-resolved spectra obtained with *s*-polarized light, using a lipid membrane containing receptor (final bulk concentration 12.8 nM) as described in Fig. 1 (*curve 1*). *Curves 2* and *3* were obtained 20 s and 60 s after the addition of 7 nM agonist to the CPWR sample cell, respectively. (*Inset*) Resonance position shift as a function of time after the addition of agonist.

changes in more detail, taking into account alterations of all three spectral parameters (i.e., resonance position, depth, and width). Such an analysis (see next section) yields the optical parameters of the system, which can be used in a quantitative characterization of the receptor-ligand binding processes.

Structural consequences of receptor incorporation and ligand binding

Characterization of the receptor-containing lipid membrane

Quantitative analysis of the plasmon resonance spectra obtained during receptor incorporation can be accomplished by fitting theoretical curves to the experimental spectra (see Fig. 1). Fig. 7 shows plots of the optical parameters obtained from such a procedure (n (Fig. 7 *A*) and t and A_n (Fig. 7 *B*); see Experimental Procedures for parameter definitions) as a function of added receptor. The solid lines are single hyperbolic curves fitted to the data points. These results indicate the following: 1) The process of receptor incorporation is satisfactorily fit by a simple Langmuir isotherm. 2) The low value of the apparent insertion constant ($\approx$14 nM) argues for a quite high efficiency of incorporation. 3) The extrapolated thickness value (6.8 nm) describes the dimension of the incorporated protein molecule perpendicular to the membrane plane (i.e., the distance between the external loops plus bound water on both sides of the membrane). Extrapolation of the refractive index curves to infinite receptor concentration (Fig. 7 *A*) results in values ($n_p\infty$ and $n_s\infty$) that characterize a monolayer of densely packed receptor molecules. From these one can calculate an average value of the refractive index (from Eq. 2) and then mass density or surface concentration (Salamon et al., 1999). From the latter value and the molecular mass of the receptor (using a molecular mass of 60 kDa), the surface area occupied by one receptor molecule can be evaluated as $S_{rec} = 1200 \pm 100$ Å^2. It is important to note that this value for the opioid receptor is in very good agreement with reported values for rhodopsin obtained with several techniques: SPR (1260 Å^2; Salamon et al., 1996), electron cryomicroscopy ($\sim$1000 Å^2; Schertler et al., 1993; Unger and Schertler, 1995), and a rhodopsin Langmuir-Blodgett film with x-ray scattering ($\sim$1100 Å^2; Maxia et al., 1995). 4) The increase in the proteolipid membrane anisotropy occurring during the process of receptor incorporation (shown in Fig. 7 *B*) clearly reflects a corresponding increase of the average long-range molecular order in the membrane resulting from receptor-lipid interactions.

Characterization of the receptor-ligand interactions

In general, CPWR spectral changes obtained with an optically anisotropic thin proteolipid membrane (i.e., changes in position, depth, and width) are the result of both mass density (molecular packing density) and structural alterations occurring within the system (for details see Salamon et al., 1999; Salamon and Tollin, 1999a,b). The mass density changes are directly reflected by the average value of the refractive index changes (see Eq. 2), whereas structural alterations will influence the refractive index anisotropy because of changes in the orientational order of molecules within the membrane. The latter quantity can be measured by changes in the refractive index values obtained with *p*- and *s*-polarized light (see Eq. 1 and further discussion below). Distinguishing between these two types of changes is especially important in the case of receptors, in which the receptor-ligand interactions are thought to result in structural alterations. This distinction can be accomplished by

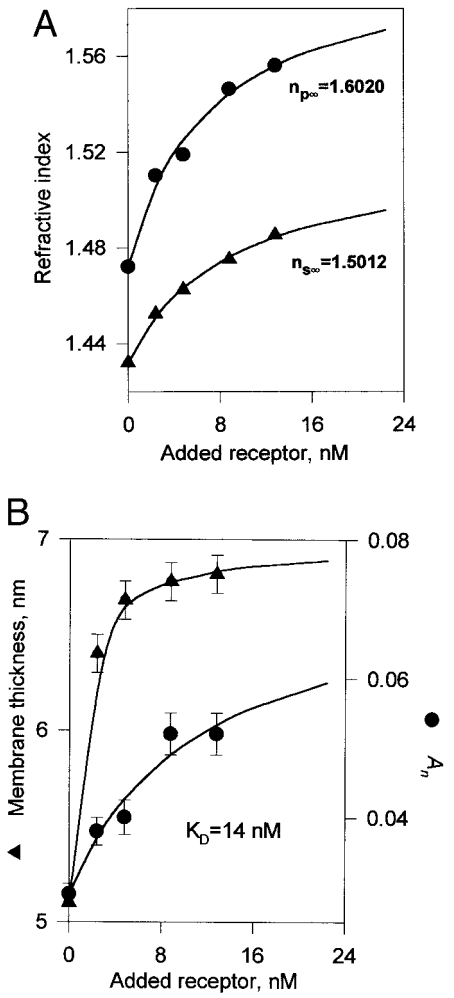

FIGURE 7 Refractive index (*A*) and thickness (*B*; ▲) values of the proteolipid film as a function of the receptor concentration, obtained from theoretical fits as described in Fig. 1. Data in *A* were obtained using either *p*- (●) or *s*- (▲) polarized light (error bars due to uncertainties in curve fitting lie within symbols). *B* also shows the refractive index anisotropy (A_n; ●) as a function of the receptor concentration. Solid lines in both panels represent nonlinear least-squares fits to a hyperbolic function. These yield limiting values of both *n* (given in figure) and *t* (6.8 nm) extrapolated to infinite concentration of the receptor, as well as an apparent binding constant K_D (given in figure).

fitting theoretical resonance curves to the experimental CPWR spectra. Using the structural parameters obtained for the receptor-containing proteolipid membrane (described in the preceding section), we have fitted theoretical resonance spectra to the experimental curves obtained in both agonist-antagonist and antagonist-agonist experiments (see Figs. 2–5). The results, expressed as changes in refractive index anisotropy, A_n, and proteolipid membrane thickness, as a function of added ligand are shown in Figs. 8 and 9, respectively.

As noted above, binding of the two ligands drives the proteolipid membrane system into distinct states characterized by different spectral characteristics (see Figs. 2–6). Based on the results in Figs. 8 and 9, one can conclude that agonist binding (either before or after antagonist binding) causes conformational changes in the receptor molecule that result in net increases in both anisotropy and mass density of the proteolipid system. The contribution of the ligand itself to these changes must be relatively small because of its small size and mass compared to the receptor and surrounding lipid molecules. Mass density increases are shown by the increased values of both n_{av} (see *inset* in Fig. 8) and *t* (preliminary experiments using another δ-opioid receptor agonist, deltorphin II, showed very similar changes in mass density, A_n, and *t* upon binding to the receptor; data not shown). In contrast, antagonist binding to the receptor induces only anisotropy changes in the system (i.e., there are no measurable changes in either n_{av} or *t* values). These conclusions are consistent with the data given in Figs. 2–5 and are especially well illustrated by the resonance position shifts shown in Fig. 4, in which the agonist induces unidirectional (i.e., *p*- and *s*-components shift in the same direction), whereas the antagonist induces bidirectional resonance position shifts. Unidirectional shifts of both spectral components in the agonist case is clear evidence of an increase in both n_p and n_s values (i.e., an increase in the average refractive index value; see Eq. 2), which occurs as a result of a mass density increase. In contrast, the addition of antagonist either before (Fig. 5) or after (Fig. 4) agonist addition does not result in mass density changes. In the latter case, all of the spectral changes are related to structural alterations. Because the two ligands have comparable molecular masses, these results must be a consequence of the addition of lipid mass to the bilayer caused by the structural changes of the receptor upon interaction with the agonist (for further discussion see below).

It is also important to note that the conformational state of the receptor induced by the antagonist has a much higher refractive index anisotropy than that produced by the agonist. This is clearly shown in both types of experiment (see Figs. 8 and 9). Thus, when the agonist is added before the antagonist, the latter ligand increases the anisotropy to almost double the value produced by the agonist. In contrast, when the agonist is added after the antagonist, the value of A_n is decreased to a level comparable to the increase produced by the agonist alone. In general, changes in refractive index anisotropy are produced by alterations in the molecular ordering with respect to the bilayer normal. In the present system, this must be a consequence of conformational changes in the receptor molecules accompanying ligand binding, i.e., changes in position and orientation of the transmembrane helices involving tilting and rotational movements, as well as movements occurring in the extramembrane loops. Changes in the acyl chain ordering of the lipid molecules induced by these protein structural alterations may also contribute.

In summary, the lack of measurable alterations in mass density or membrane thickness upon antagonist binding

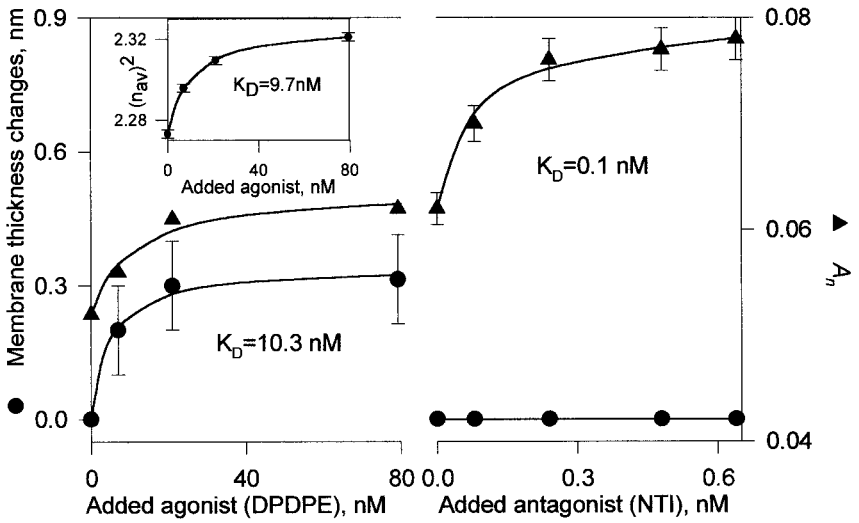

FIGURE 8 Average change in thickness (●) and refractive index anisotropy values (▲) for a proteolipid membrane containing opioid receptor (bulk concentration 12.8 nM) as a function of the agonist and antagonist concentration. Results were obtained from the experiment in Fig. 4 by theoretical fits to the experimental spectra (see Figs. 1 and 7). (*Inset*) Square of the average refractive index of the proteolipid membrane as a function of agonist concentration. Solid lines represent nonlinear least-squares fits to a hyperbolic function from which the binding constant values (K_D) were obtained. For purposes of clarity, error bars (corresponding to curve fitting errors) for circles and triangles are shown only for one of the two curves in the main panel.

implies a critical difference in the conformational changes induced by such binding compared with those induced by the agonist. This distinction is also reflected in the fact that the state of the proteolipid membrane created by the addition of antagonist before agonist is different from that created when antagonist is added after agonist. These differences arise because the agonist is able to generate structural alterations perpendicular to the plane of the membrane, changing its thickness, whereas the antagonist cannot do so. Thus the antagonist produces two substates, depending upon whether it is interacting with the unliganded receptor or with a receptor that has agonist bound to it and therefore has changed its dimensions relative to the membrane normal. Although these two substates are characterized by similar optical anisotropies, they have different dimensions and mass density. Because NTI is a pure δ receptor antagonist with no reported partial agonist biological activities (Wild et al., 1994), it is reasonable to conclude that both of these substates are inactive in signal transduction. While it is possible that the short-lived state represents the receptor state that could lead to negative intrinsic activity (Costa et al., 1992) if it were long lived enough, a more likely possibility is that the two substates represent nonequilibrium steady states (Kenakin, 1990) that are accessible to the receptor, with one of these being only transiently observed when NTI interacts with the δ receptor. To obtain further insights into these states, structural changes in the lipid and protein components must be separately determined for both agonist and antagonist binding and under a wide range of ratios of agonist to antagonist. This can be done using chromophore-labeled lipids, and such experiments are under way.

Thermodynamic values for the individual ligand dissociation constants can easily be evaluated from the hyperbolic fits to the anisotropy changes presented in Figs. 8 and 9. The results are given in Table 1. It is evident that these disso-

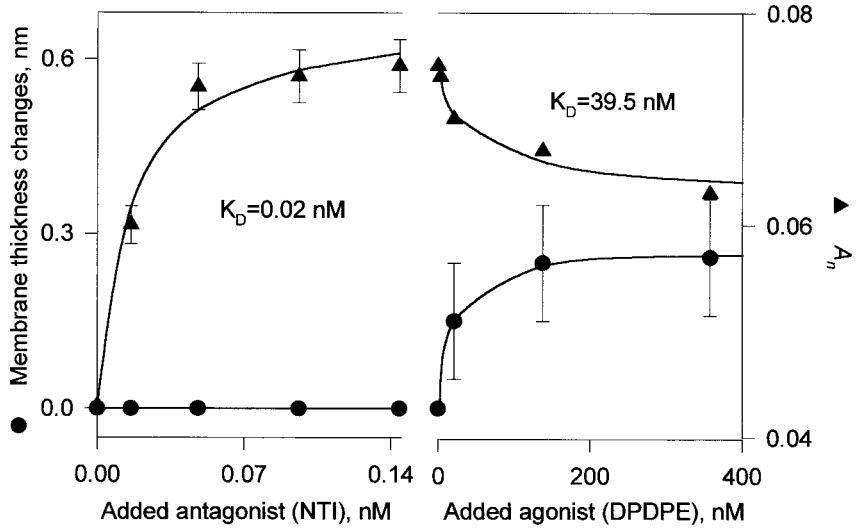

FIGURE 9 Average change in thickness (●) and refractive index anisotropy values (▲) as a function of antagonist and agonist concentration. Results were obtained from the experiment in Fig. 5 by theoretical fits to the experimental spectra. Other details are as in Fig. 8.

TABLE 1 Dissociation constant values obtained for DPDPE and NTI from experiments described in Figs. 8 and 9

	DPDPE K_D (nM)	NTI K_D (nM)
DPDPE added first	10.0 ± 0.4*	0.10 ± 0.01†
NTI added first	40.0 ± 0.4‡	0.020 ± 0.005§

*No NTI present.
†Obtained in the presence of 80 nM DPDPE.
‡Obtained in the presence of 0.14 nM NTI.
§No DPDPE present.

ciation constants strongly depend on whether the agonist is present when the antagonist is added, and vice versa. Thus the presence of the other ligand causes an appreciable shift of K_D to higher values. This observation is especially significant in the present system, in which the antagonist has a much higher binding affinity than the agonist (by two to three orders of magnitude). Despite this, when NTI is added after DPDPE, its dissociation constant increases significantly (about fourfold). This finding cannot be simply explained by competition between these two ligands. We conclude that this constitutes another indication that different conformational states are induced by these ligands, which are characterized by different binding constants for the other ligand.

The binding constants determined here for DPDPE and NTI are similar to those reported in the literature, using a variety of δ-opioid receptor membrane preparations and a variety of radiolabeled competitive ligands. For DPDPE, some typical values reported in the literature include 3.3–5.2 nM in several rat brain membrane preparations (Akiyama et al., 1985), 1.2 nM for the receptor cloned into the NG-108-15 cell line (Akiyama et al., 1985), and 85 nM for the receptor cloned into the Chinese hamster ovary cell line (unpublished data). Thus the K_D values of 10–40 nm reported here are consistent with those expected for a fully functional receptor. Likewise, the K_D values previously reported (Wild et al., 1994) for NTI (0.9 nM in NG-108-15 cloned receptors, 0.13 nM in mouse brain membranes, and 0.15 nM in mouse spinal chord preparations) are consistent with the values of 0.02–0.10 nM reported here.

Structural basis of receptor function

The CPWR results presented in this paper demonstrate the formation of several conformational states of the proteolipid membrane as a consequence of receptor-agonist and receptor-antagonist interactions. In the case of agonist binding, the slow multiphasic kinetics clearly indicate that there are a number of intermediate conformational states involved in the formation of the final activated state, as has been suggested by Gether and Kobilka (1998). It is not clear at present whether this final state involves an equilibrium mixture of different conformational forms of the receptor, or preferential formation of one particular receptor structure (Kenakin, 1995). In either case, the present study has shown that the receptor-agonist conformation produces an elongation of the receptor molecule (an increase in t), as well as an overall increase in the degree of orientational order of molecules within the membrane (an increase in refractive index anisotropy, A_n). It is reasonable to expect this process to be relatively slow because it also involves alterations in the lipid phase of the membrane in response to receptor elongation. Based on models for opioid receptor structural changes upon activation (Pogozheva et al., 1998; Knapp et al., 1995; Gether and Kobilka, 1998), derived from studies of rhodopsin (Farrens et al., 1996), bacteriorhodopsin (Luecke et al., 1999), and the β-adrenergic receptor (Gether and Kobilka, 1998), we suggest that the elongation process involves tilting and rotation of one or more of the transmembrane helices, resulting in vertical movements of the extramembrane loops, and is accompanied by movement of lipid molecules that cause an increase in the positive curvature of the lipid surface. The increase in curvature also requires the movement of lipid molecules from the plateau-Gibbs border to the bilayer phase, which increases the overall surface mass density of the proteolipid membrane. The anisotropy changes can be ascribed predominantly to orientation changes of the transmembrane helices that influence the ordering of the hydrocarbon chains of lipid molecules, without a significant contribution from the extracellular loops or lipid mass redistribution. In contrast, the binding of antagonist results only in an increase in the refractive index anisotropy, which implies localized alterations occurring within the receptor molecule that are restricted to transmembrane helix and lipid hydrocarbon chain orientation. The schematic model shown in Fig. 10 represents an attempt to visualize the structural consequences of δ-opioid receptor interaction with either agonist or antagonist based on these observations. Such a multistate model allows a simple explanation of the well-known fact that competitive antagonists, although they occupy the same binding site in the receptor as agonists, do not transduce signals across the proteolipid membrane.

A more complete understanding of the molecular mechanisms of receptor-ligand interactions will require more detailed information about the structural changes induced in the receptor by different classes of ligands. In particular, further time-resolved studies are needed to characterize the sequence of conformational changes associated with the intermediate states that follow ligand binding. It will also be important to increase our knowledge of the effects of lipid membrane structure, salt concentration, pH, other ligands such as allosteric effectors, and other proteins (e.g., G-proteins, kinases, etc.) on the formation of the liganded states of the receptor. The present studies have shown that CPWR spectroscopy provides a new and powerful experimental tool for such investigations, for GPCRs as well as other membrane-bound receptors, enzymes, ion channels,

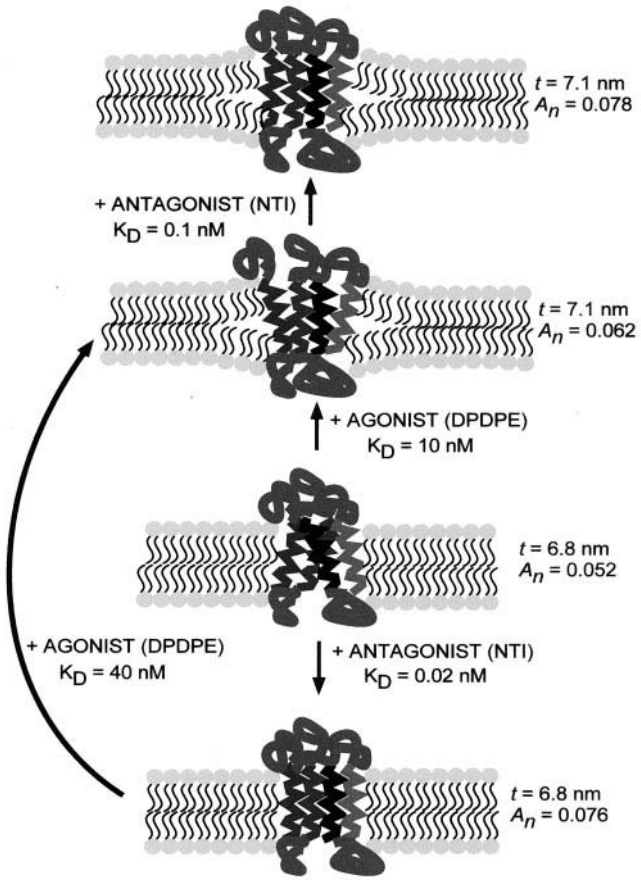

FIGURE 10 Schematic representation of changes in conformation (evaluated by refractive index anisotropy and membrane thickness values) and mass distribution (evaluated by membrane thickness and average refractive index values) of lipid and receptor molecules during interaction of the receptor with either agonist or antagonist molecules. For clarity, only four of the transmembrane helices and the extramembrane loops of the receptor are shown. Structural transitions occurring upon the addition of agonist subsequent to antagonist addition, and the addition of antagonist subsequent to agonist addition, are also shown. See text for further description.

etc. In addition, the methods reported here should be readily adaptable to high-throughput screening, in view of the minute amounts of receptor and ligand needed for a complete dose-response binding assay and for evaluation of receptor structural changes.

This work was supported in part by grants from the Vice President for Research, University of Arizona (to GT and VJH), the National Science Foundation (MCB-9904753) (to GT and ZS), the U.S. Public Health Service, and the National Institute of Drug Abuse (DA-06284) (to VJH), and a U.S. Public Health Service Postdoctoral Fellowship (DA-05787) (to SC).

REFERENCES

Akiyama, K., K. W. Gee, H. I. Mosberg, V. J. Hruby, and H. I. Yamamura. 1985. Characterization of [^{3}H] [2-D-penicillamine, 5-D-penicillamine]-enkephalin binding to δ opiate receptors in the rat brain and neuroblastoma-glioma hybrid cell line (NG108-15). *Proc. Natl. Acad. Sci. USA.* 82:2543–2547.

Born, M., and E. Wolf. 1965. Principles of Optics. Pergamon Press, New York.

Costa, T., Y. Ogino, P. J. Munson, H. O. Onaran, and D. Rodbard. 1992. Drug efficacy at guanine nucleotide-binding regulatory protein-linked receptors: thermodynamic interpretation of negative antagonism and receptor activity in the absence of ligand. *Mol. Pharmacol.* 41:290–297.

Cuypers, P. A., J. W. Corsel, M. P. Janssen, J. M. M. Kop, W. Th. Hermens, and H. C. Hemker. 1983. The adsorption of prothrombin to phosphatidylserine multilayers quantitated by ellipsometry. *J. Biol. Chem.* 258:2426–2431.

Farrens, D. L., Ch. Altenbach, K. Yang, W. L. Hubbell, and H. G. Khorana. 1996. Requirement of rigid-body motion of transmembrane helices for light activation of rhodopsin. *Science.* 274:768–770.

Gether, U., and B. K. Kobilka. 1998. G-protein-coupled receptors. *J. Biol. Chem.* 273:17979–17982.

Gether, U., S. Lin, P. Ghanouni, J. A. Ballesteros, H. Weistein, and B. K. Kobilka. 1997. Agonist induce conformational changes in transmembrane domains III and VI of the β_2 adrenoceptor. *EMBO J.* 16: 6737–6747.

Gimpl, G., J. Anders, C. Thiele, and F. Fahrenholz. 1996. Photoaffinity labeling of the human brain cholecystokinin receptor overexpressed in insect cells. *Eur. J. Biochem.* 237:768–777.

Grisshammer, R., and J. Tucker. 1996. Purification of a rat neurotensin receptor expressed in *Escherichia coli. Biochem. J.* 317:891–899.

Kenakin, T. 1990. Drugs and receptors: an overview of the current state of knowledge. *Drugs.* 40:666–687.

Kenakin, T. 1995. Agonist-receptor efficacy II: agonist trafficking of receptor signals. *Trends Pharmacol. Sci.* 16:232–238.

Knapp, R. J., E. Malatynska, N. Collins, L. Fang, J. Y. Wang, V. J. Hruby, W. R. Roeske, and H. I. Yamamura. 1995. Molecular biology and pharmacology of cloned opioid receptors. *FASEB J.* 9:516–525.

Knapp, R. J., E. Malatynska, L. Fang, L. Xiaoping, M. Nguyen, G. Santoro, E. V. Varga, V. J. Hruby, W. R. Roeske, and H. I. Yamamura. 1994. Identification of a human delta opioid receptor: cloning and expression. *Life Sci.* 54:PL463–PL469.

Korlipara, V. L., A. E. Takemori, and P. S. Portoghese. 1995. Electrophilic N-benzylnaltrindoles as delta-opioid receptor-selective antagonists. *J. Med. Chem.* 38:1337–1343.

Luecke, H., B. Schobert, H. T. Richter, J. Ph. Cartailler, and J. K. Lanyi. 1999. Structural changes in bacteriorhodopsin during ion transport at 2 angstrom resolution. *Science.* 286:255–260.

Maxia, L., G. Radicchi, I. M. Pepe, and C. Nicolini. 1995. Characterization of Langmuir-Blodgett films of rhodopsin: thermal stability studies. *Biophys. J.* 69:1440–1446.

Mosberg, H. I., R. Hurst, V. J. Hruby, K. Gee, H. I. Yamamura, J. J. Galligan, and T. F. Burks. 1983. Bis-penicillamine enkephalins possess highly improved specificity toward delta opioid receptors. *Proc. Natl. Acad. Sci. USA.* 80:5871–5874.

Mueller, P., D. O. Rudin, H. T. Tien, and W. C. Wescott. 1962. Reconstitution of cell membrane structure in vitro and its transformation into an excitable system. *Nature.* 194:979–980.

Okura, T., S. M. Cowell, E. Varga, T. H. Burkey, W. R. Roeske, V. J. Hruby, and H. I. Yamamura. 2000. Differential down regulation of the human δ-opioid receptor by SNC80 and [D-Pen2, D-pen5]enkephalin. *Eur. J. Pharmacol.* 387:R11–R13.

Pogozheva, I. D., A. L. Lomize, and H. I. Mosberg. 1998. Opioid receptor three- dimensional structures from distance geometry calculations with hydrogen bonding constraints. *Biophys. J.* 75:612–634.

Quock, R. M., T. H. Burkey, E. Varga, Y. Hosohata, K. Hosohata, S. M. Cowell, C. A. Slate, F. J. Ehlert, E. R. Roeske, and H. I. Yamamura. 1999. The δ-opioid receptor: molecular pharmacology, signal transduction, and the determination of drug efficacy. *Pharmacol. Rev.* 51: 503–531.

Raynor, K., H. Kong, Y. Chen, K. Yasuda, L. Yu, G. I. Bell, and T. Reisine. 1994. Pharmacological characterization of the cloned κ-, δ- and μ-opioid receptors. *Mol. Pharmacol.* 45:330–334.

Salamon, Z., M. F. Brown, and G. Tollin. 1999. Plasmon resonance spectroscopy: probing molecular interactions within membranes. *Trends Biochem. Sci.* 24:213–219.

Salamon, Z., D. Huang, W. A. Cramer, and G. Tollin. 1998. Coupled plasmon- waveguide resonance spectroscopy studies of the cytochrome b_6f/plastocyanin system in supported lipid bilayer membranes. *Biophys. J.* 75:1874–1885.

Salamon, Z., G. Lindblom, L. Rilfors, K. Linde, and G. Tollin. 2000. Interaction of phosphatidylserine synthase from *E. coli* with lipid bilayers: coupled plasmon-waveguide resonance spectroscopy studies. *Biophys. J.* 78:1400–1412.

Salamon, Z., H. A. Macleod, and G. Tollin. 1997a. Coupled plasmon-waveguide resonators: a new spectroscopic tool for probing proteolipid film structure and properties. *Biophys. J.* 73, 2791–2797.

Salamon, Z., H. A. Macleod, and G. Tollin. 1997b. Surface plasmon resonance spectroscopy as a tool for investigating the biochemical and biophysical properties of membrane protein systems. I. Theoretical principles. *Biochim. Biophys. Acta.* 1331:117–129.

Salamon, Z., and G. Tollin. 1999a. Surface plasmon resonance: theory. *In* Encyclopedia of Spectroscopy and Spectrometry, Vol. 3. J. C. Lindon, G. E. Tranter, and J. L. Holmes, editors. Academic Press, San Diego. 2311–2319.

Salamon, Z., and G. Tollin. 1999b. Surface plasmon resonance: applications. *In* Encyclopedia of Spectroscopy and Spectrometry, Vol. 3. J. C. Lindon, G. E. Tranter, and J. L. Holmes, editors. Academic Press, San Diego. 2294–2302.

Salamon, Z., and G. Tollin. 2000. Surface plasmon resonance spectroscopy in peptide and protein analysis. *In* Encyclopedia of Analytical Chemistry. R. A. Meyers, editor. Wiley, New York. In press.

Salamon, Z., Y. Wang, M. F. Brown, A. H. Macleod, and G. Tollin. 1994. Conformational changes in rhodopsin probed by surface plasmon resonance spectroscopy. *Biochemistry.* 33:13706–13711.

Salamon, Z., Y. Wang, J. L. Soulages, M. F. Brown, and G. Tollin. 1996. Surface plasmon resonance spectroscopy studies of membrane proteins: transducin binding and activation by rhodopsin monitored in thin membrane films. *Biophys. J.* 71:283–294.

Schertler, G. F. X., C. Villa, and R. Henderson. 1993. Projection structure of rhodopsin. *Nature.* 362:770–772.

Unger, V. M., and G. F. X. Schertler. 1995. Low resolution structure of bovine rhodopsin determined by electron cryo-microscopy. *Biophys. J.* 68:1776–1786.

Wild, K. D., F. Porreca, H. I. Yamamura, and R. B. Raffa. 1994. Differentiation of receptor subtypes by thermodynamic analysis. Application to opioid δ receptors. *Proc. Natl. Acad. Sci. USA.* 91:12018–12021.